Noise Radar Electronic Protection and Spectrum Sharing Field Test

Kai Hiltunen and Jouni Malinen
Patria Aviation Oy
Hatanpään valtatie 30
FI-33100 TampereFINLAND

kai.hiltunen@patriagroup.com

jouni.malinen@patriagroup.com

ABSTRACT

In this paper we present results from a field test of a continuous wave noise radar. The purpose of the test was to evaluate the performance of the radar in a signal environment where interfering signals are present. Two waveforms were used as interfering signals: frequency swept pulse signal and band limited gaussian noise. The first signal type represents a type of unintentional interference that may occur in the radar frequency band and the second signal type represents an intentional jamming signal. By using digital signal processing methods, the noise radar was successfully operated in signal environment where another radar signal or jamming signal was present.

1.0 INTRODUCTION

A wideband continuous wave noise radar can offer advantages like high range resolution and low transmit signal spectral power density and hence low probability of intercept. In congested frequency bands the wideband operation is only possible if the wideband radar can tolerate the other spectrum users sharing the same band. The other users can be for example other radars or intentional jamming.

As a part of a two-year study on noise radars a field test was performed to study the electronic protection methods and the performance of a noise radar in a spectrum sharing scenario. The interference and jamming signals in the measurements were a conventional linear frequency modulated pulse radar and continuous noise waveform used as a jamming signal.

Because the radar itself was a monostatic continuous wave noise radar, the radar processing included the self-interference and adaptive clutter cancellation. When the interference or jamming was present, additional processing steps were needed to reach the nominal sensitivity of the radar. In this field test setup, the level of the interfering signals was low enough so that the receiver was not saturated. This kind of scenario is relevant especially in multistatic noise radar systems, where the locations of the receivers are not known, and it is hence difficult to focus the jamming to the receiver sites. The processing principles presented in this article can be used in a modern, resilient multistatic noise radar system even though these field tests were performed in a monostatic configuration.

2.0 MEASUREMENT SETUP

The measurement setup is shown in Figure 1. The transmitter and receiver antennas were mounted on two different poles about 1.5 meters from each other. The antenna for the jammer or the interfering transmitter was located about ten meters away from the radar antennas. Cars travelling on a road at about 200-400 meters distance from the radar were the targets of the interest in this measurement.

The transmit antenna was an evenly fed patch antenna array having 2x6 elements. The receiver antenna was made of similar patch antennas so that the width of the array was 3 elements and height 6 elements. The elements on top of each other were evenly fed by using a fixed power combiner network resulting in a three-element horizontal, linear array. The three antenna elements were connected to separate receiver channels allowing beamforming operation. The antenna for the jammer or interfering transmitter was a wideband horn antenna. All the antennas in this measurement setup were horizontally polarized.

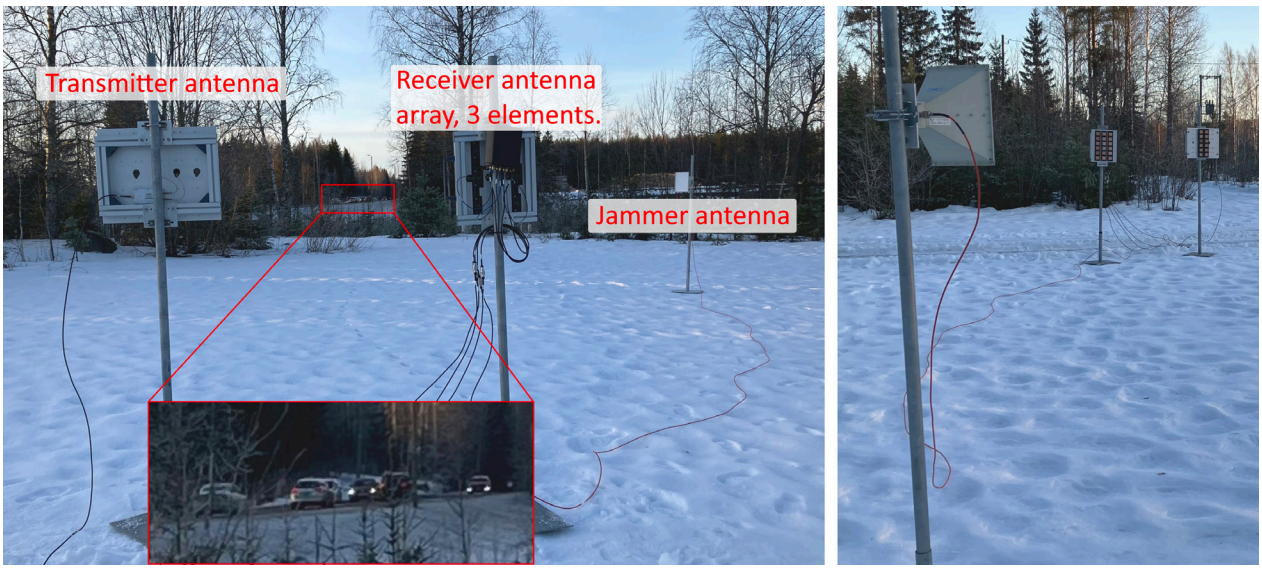

Figure 1: Field measurement setup.

The transmitter, which was used in the field test was based on a two-channel RF sampling D/A-converter evaluation system. The first channel of the D/A-converter was used for generating the radar waveform and the second channel was used for the jamming and interfering signal generation. The D/A-converter generated the signals directly to the radar operating frequency of 2.88 GHz. Signal chain between the D/A-converter and the antenna consisted of an amplifier, a lowpass filter and a directional coupler, which was used to take a sample of the transmitted signal to the reference channel of the radar receiver.

The receiver in the test was USRP X300 with two TwinRX daughter cards, so that the total number of coherent channels was four. One channel was used for the reference signal reception from the directional coupler and the other three channels for the receiver antenna signals. The receiver system included also a three-channel low noise amplifier and coaxial cables between the preamplifier and the receiver. The receiver gain setting was adjusted so that the total noise figure of the receiver system was about 6 dB. The transmit power was adjusted so that the radar transmit signal leaking to the receiver was close to the full-scale level of the receiver. The block diagram of the measurement system is presented in Figure 2.

The radar signal waveform used in the test was a frequency modulated signal having constant envelope. The modulating signal was generated so that a nonlinear operation was applied to compress the values of the gaussian random samples. The purpose of this operation was to shape the spectrum and the autocorrelation function of the waveform so that the spectrum became wider and autocorrelation main lobe narrower than without the compression. The bandwidth of the noise radar signal was about 60 MHz, so that it fits to the receiver maximum bandwidth of 80 MHz. The jammer signal in the test was band-limited gaussian white noise having bandwidth of 20 MHz. The other interfering signal was a pulse radar signal. The signal waveform imitated the civilian air traffic control radar, which is used in Helsinki-Vantaa airport. The transmit power of the jamming and interfering signals were set so that they were approximately equal to the level of the radar signal leaking from the transmitter to the receiver.

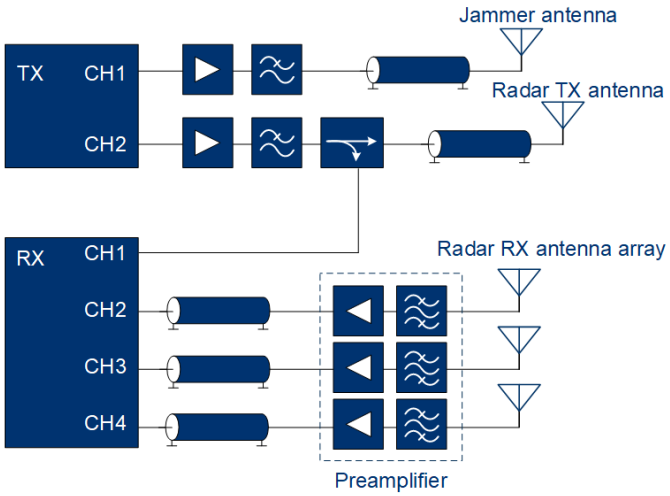

Figure 2: Block diagram of the measurement system.

3.0 MEASUREMENT RESULTS

Sensitivity of a monostatic continuous wave noise radar is challenged by the strong transmit signal leakage from the transmitter to the receiver and the strong ground clutter echoes from the vicinity of the radar. Transmit signal leakage can be mitigated by designing transmitting and receiving antennas so that the isolation between the antennas is optimized. The ground clutter on the other hand can be attenuated by using adaptive cancellation methods in the radar signal processing. In these measurements the least squares method was used to estimate and cancel the ground clutter. The efficiency of the matrix algebra computing was enhanced by exploiting the matrix symmetries [1].

Figure 3(a) presents the spectrum of the various signals when there is no interference or jamming present. The red trace shows the spectrum of the target channel signal. The total power in the target channel is about -65 dBm. The blue trace is the spectrum for the processed signal after the adaptive clutter cancellation. The figure also includes the black spectrum trace for the case where the antenna was replaced with a matched termination. The black trace hence presents the thermal noise of the measurement system. The receiver system was calibrated so that the power spectral density at the center frequency presents the true, calibrated value. As can be seen from the figure, the adaptive clutter cancellation reduces the signal level on the radar target channel to the thermal noise level. The residual total noise power over the whole operating band is about -90 dBm, meaning that the clutter cancellation was about 25 dB.

In the next case, in Figure 3(b), the noise jamming is present. Just like in the previous figure the red trace presents the target channel signal. In this case the clutter cancellation reveals the jamming signal (blue trace). The total power on the channel after the first cancellation step is about -73 dBm, i.e. about 17 dB higher than in the previous case without the jamming signal. So, in this case the radar loses about 17 dB of its sensitivity due to the jamming signal if no further processing steps are taken. After the first cancellation it is possible to measure the direction of arrival for the jamming signal. It is also possible to use beamforming to create a “reference” signal of the jamming signal. This “reference” signal was used in the second adaptive cancellation step. The spectrum trace after the second cancellation step is presented in Figure 3(b) with green trace. As can be seen from the figure, the target channel spectral power density after the second cancellation step is close to the thermal noise power density, meaning that the radar can operate at the same sensitivity level as in the case where the jamming signal was not present.

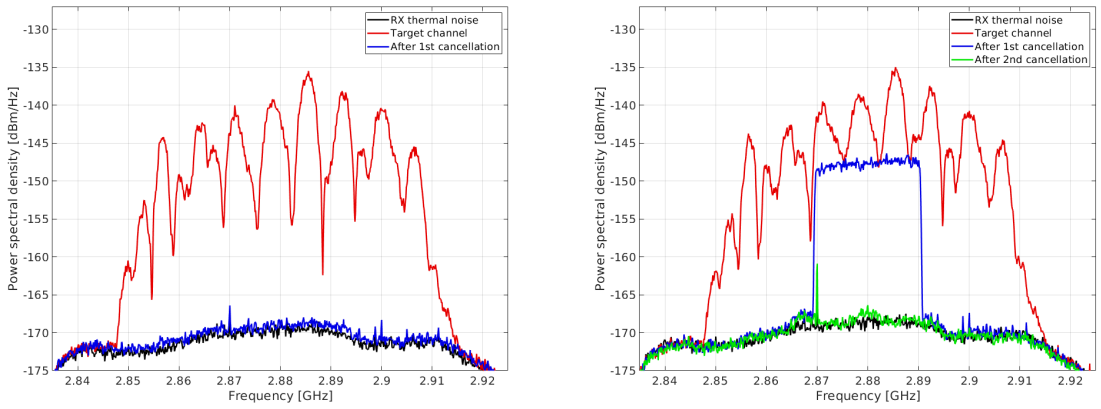

(a) (b)

Figure 3: Signal spectra when (a) no jammer is present and (b) 20 MHz wide noise jammer is present.

The effect of the second cancellation step in the radar range-doppler view is presented in Figure 4. In addition to the range-doppler matrices the figure also shows one crosscut of the range-doppler matrix at the speed of 21 m/s. During the measurement there was a truck at about 150 m distance traveling at that speed. Figure 4(a) presents the case where only the first cancellation step is performed and the Figure 4(b) the case where two cancellation steps are performed. Because the second cancellation step decreased the residual noise and interference power on the target channel about 17 dB, as was mentioned above, the same improvement can also be seen from the range-doppler results: the SINR of the truck detection is improved about 17 dB.

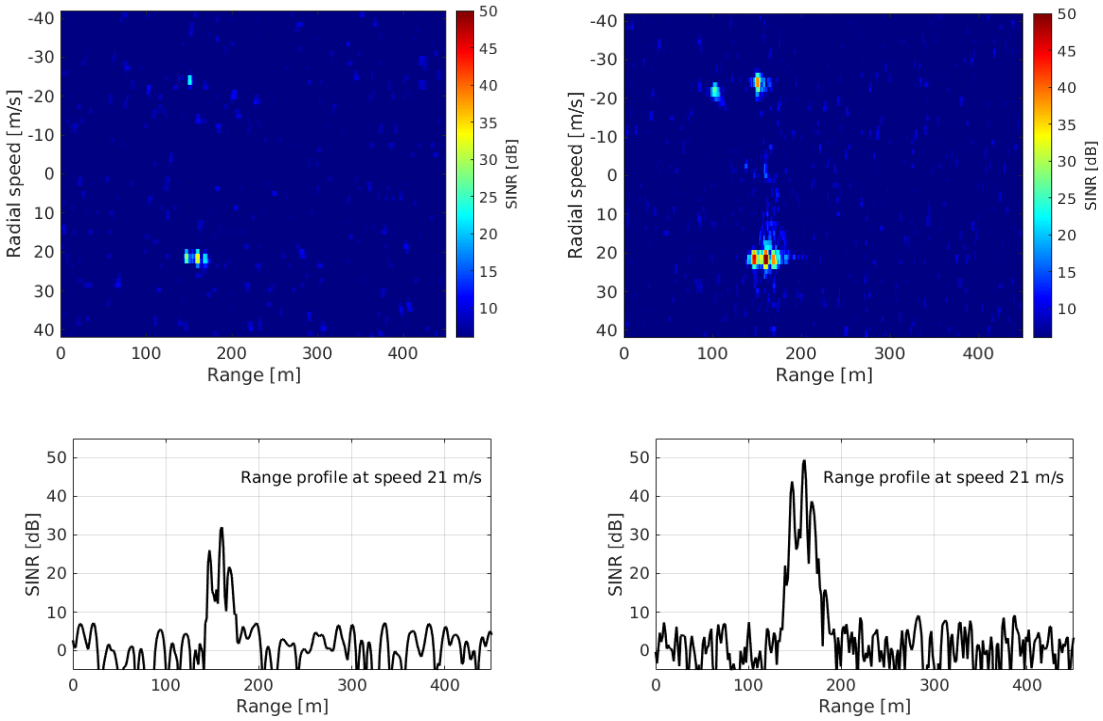

(a) (b)

Figure 4: Range-doppler display in noise jamming situation. (a) Clutter cancellation only, (b) Clutter and jammer cancellation.

In the second test case the interfering signal was a pulse radar signal. Similar spectrum traces as in the previous figures are presented for the pulse radar interference case in Figure 5(a). It should be noted that the spectrum traces in this figure are so called "max hold" traces so that the pulsed interference signal is better shown in the figure. This also means that the power spectral density values for the noise level is about 10 dB higher than in Figure 3, which presented the average power spectral density. Because the bandwidth of the pulse signal is only about 6 MHz, it has higher power spectral density than the previous noise jamming signal and it can be seen in the target channel spectrum also before the adaptive clutter cancellation. After the cancellation the situation is the same as in the jamming signal case: only the interfering signal and thermal noise is remaining on the target channel. The signal after the clutter cancellation can also be presented in time domain as in Figure 5(b). In the time domain figure the pulses are clearly observable as well as the shape of the main beam for the interfering radar signal. In the field test the antenna of the interfering transmitter was a fixed horn antenna. The shape of the main beam and antenna scanning was emulated in this test by modulating the amplitude of the transmitted signal samples.

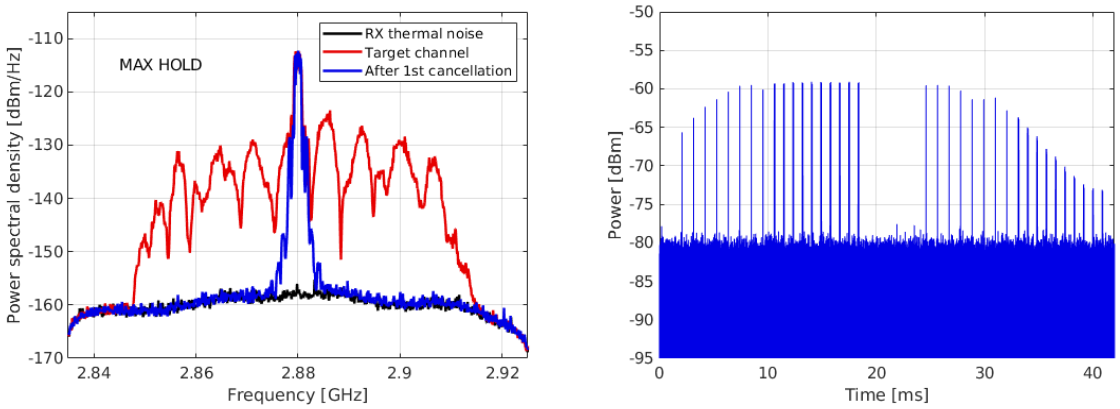

Figure 5: Pulse radar interference (a) spectrum and (b) in time domain.

Because the radar signal waveform is wideband and continuous on the contrary to the interfering signal, which is a narrowband pulse signal, it is possible to maintain most of the processing gain of the noise radar even though some of samples are contaminated by the interfering signal. The radar processing can be done by attenuating the interfering signal by filtering in frequency domain or by saturating the sample values, which include the strong pulse interference, in time domain. Referring to Figure 5 the frequency domain filtering would mean creating a 6 MHz wide notch filter at the frequency of 2.88 GHz and the sample value saturation would mean saturating the signal samples, which exceed the power of about -78 dBm. Saturation was performed by hard clipping the sample values to this maximum power. Instead of hard clipping it would also be possible to use other nonlinear functions to saturate the sample values [2], but in this test the hard clipping seemed to provide adequate results.

Attenuating a narrowband pulse signal either by filtering or by saturating the sample values does not require much computing resources. These operations enable the radar operation near the nominal sensitivity level but may cause some artefacts to the radar range-doppler matrix. A narrowband pulse signal interference can also be attenuated in similar fashion as the wideband noise interference in the previous case. Adaptive filtering can be used to attenuate the pulse interference by directing the receiver antenna array towards the source of the pulse interference and using that signal as a "reference" in the adaptive filtering.

Figure 6 presents the radar range-doppler matrices for the various test cases with the interfering pulse signal. In the first case (Figure 6(a)) only the ground clutter cancellation is performed, and the interfering signal

significantly reduces the sensitivity of the radar compared to the other three cases (Figure 6(b) - Figure 6(d)). This can be seen by observing that the SINR values of the two strong targets at about 200 m and 20 m/s are much lower and the weak targets at about 350-400 meters range and speeds -20 m/s and 20 m/s cannot be detected in Figure 6(a). In the other three cases the SINRs of the targets are very similar and the radar can operate near its nominal sensitivity level despite the interfering signal. There are, however, some differences in the range-doppler figures. Filtering out the frequencies of the interfering signal generates strong correlation sidelobes in the range axis and makes it more difficult to separate the two strong targets at about 200 m range and 20 m/s speed. Saturating the signal samples in time domain on the other hand generates sidelobes in doppler (speed) direction. The sidelobes are not as strong as in the frequency filtering case but the sidelobe peaks can be observed at about -38 m/s speed at the same range as the strong target echoes. The doppler distance between the main lobe and the sidelobe peak is equal to the pulse repetition frequency of the interfering radar signal. The adaptive filtering requires more computing resources than frequency filtering or sample saturation, but it does not generate sidelobes to the range-doppler matrix as can be seen in the Figure 6(d).

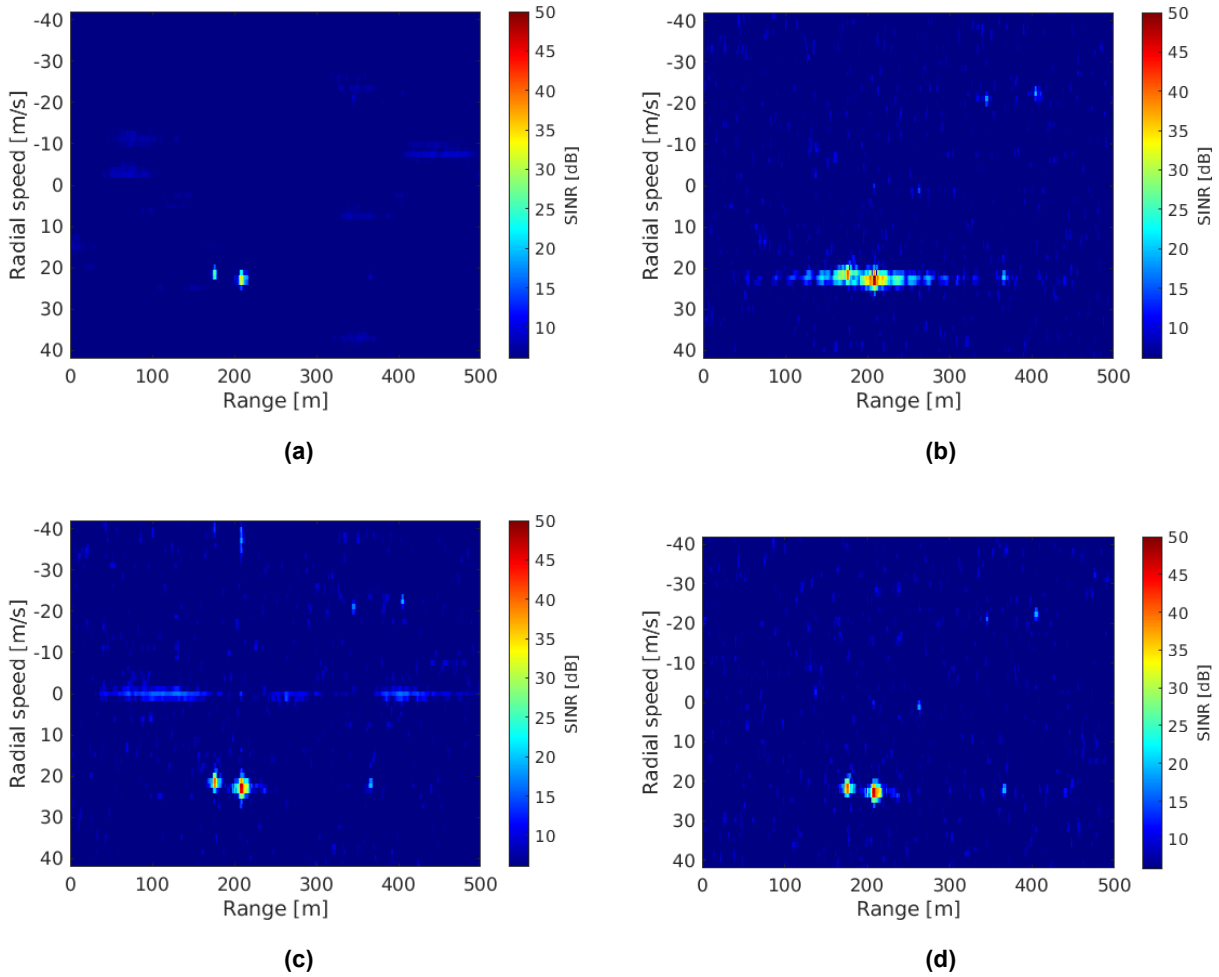

Figure 6: Range-doppler view for different interference processing: clutter cancellation and (a) no other steps, (b) filtering of the interference (c) saturation of the interference and (d) adaptive filtering of the interference.

4.0 CONCLUSIONS

This field test was performed to analyse the performance of a continuous wave noise radar in a situation where unintentional interference or intentional jamming signal is present. The interfering signal was either a pulse radar signal or a continuous wave noise jamming signal. It was shown that the noise radar can operate near its nominal sensitivity level despite the interference by using adaptive filtering. For a narrowband pulse interference, it is also possible to use frequency domain filtering or time domain sample saturation, which require less processing resources than the adaptive filtering. These low complexity methods may, however, generate some artefacts to the range-doppler matrix measured by the radar. In this field test the level of the interfering signals was low enough so that receiver can operate in linear region and attain low noise figure. This is a realistic scenario especially for a multistatic noise radar where the locations of the receiver nodes are not known, and the jamming can not be focused to the directions of the receivers. The processing principles presented in this article can be used in a modern, resilient multistatic noise radar system even though these field tests were performed in a monostatic configuration.

5.0 REFERENCES

[1] M. Meller, “Efficient Signal Processing Algorithms for Passive Radars”, in Meeting Proceedings STO-MP-SET-187, May 2013.

[2] M. Malanowski and K. Kulpa, “Robust detection in continuous-wave noise radar – experimental results,” 11-th International Radar Symposium, Vilnius, Lithuania, 2010, pp. 1-4.